Journal Pre-proofs

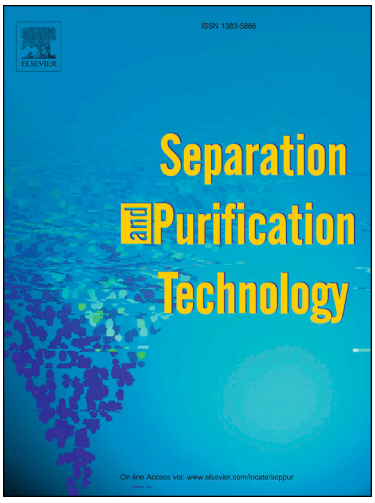

Recovery of platinum from spent automotive catalytic converters by leaching with aluminium-based salts solutions

Flavia N. Braga, António Coelho, Ana R.F. Carreira, Filipe H.B. Sosa, Nicolas Schaeffer, Helena Passos, João A.P. Coutinho

PII: S1383-5866(25)02600-0
DOI: https://doi.org/10.1016/j.seppur.2025.134003
Reference: SEPPUR 134003

To appear in: *Separation and Purification Technology*

Received Date: 11 March 2025
Revised Date: 14 May 2025
Accepted Date: 13 June 2025

Please cite this article as: F.N. Braga, A. Coelho, A.R.F. Carreira, F.H.B. Sosa, N. Schaeffer, H. Passos, J.A.P. Coutinho, Recovery of platinum from spent automotive catalytic converters by leaching with aluminium-based salts solutions, *Separation and Purification Technology* (2025), doi: https://doi.org/10.1016/j.seppur.2025.134003

Recovery of platinum from spent automotive catalytic converters by leaching with aluminium-based salts solutions

Flavia N. Braga[a,b,c], António Coelho[a], Ana R. F. Carreira[a], Filipe H. B. Sosa[a], Nicolas Schaeffer[a,*], Helena Passos[b,c,*], João A.P. Coutinho[a]
[a]CICECO - Aveiro Institute of Materials, Department of Chemistry, University of Aveiro, 3810-193 Aveiro, Portugal
[b]LSRE-LCM – Laboratory of Separation and Reaction Engineering – Laboratory of Catalysis and Materials, Faculty of Engineering, University of Porto, Rua Dr. Roberto Frias, 4200-465 Porto, Portugal
[c]ALiCE – Associate Laboratory in Chemical Engineering, Faculty of Engineering, University of Porto, Rua Dr. Roberto Frias, 4200-465 Porto, Portugal
*Corresponding authors: hpassos@fe.up.pt; nicolas.schaeffer@ua.pt

Abstract
The increasing global demand for metals has intensified mining activities, raising serious environmental concerns. Platinum group metals (PGM), classified as critical raw materials (CRM) by the European Union, are essential to modern industries, particularly for automotive catalytic converters. Recycling PGM from spent automotive catalytic converters (SACC) represents a sustainable and circular economy strategy, reducing the dependence on primary mining. In this study, a new hydrometallurgical process was developed for PGM recovery from SACC using an aqueous solution of $AlCl_3 \cdot 6H_2O$ and $Al(NO_3)_3 \cdot 9H_2O$ which offers a greener alternative to the harsh *aqua regia*. A real SACC from a diesel vehicle was used, following its characterization and pretreatment. The characterization confirmed that Pt was the only measurable PGM present in its composition. Key leaching operational parameters, including reagents and solid-to-liquid (S/L) ratios, temperature, and contact time, were optimized, with temperature identified as the critical factor for Pt leaching. Under optimal conditions, the single-step leaching process demonstrated high efficiency, achieving 94% of Pt extraction. The selective separation of Pt was achieved using the Ambersep 900® anion-exchange resin, followed by Pt elution with a thiourea solution. The process was successfully scaled up 60-fold, demonstrating leaching media reusability over five cycles without loss of efficiency and achieving a Pt concentration of 418 $mg \cdot L^{-1}$. The resin adsorbed 97% of Pt, with 96% recovery during the desorption step, finally obtaining Pt isolated. A preliminary cost analysis highlights the economic viability of this acid-free recovery method.

Keywords:
Circular economy, Critical metals, Hydrometallurgy, Recycling, Waste valorisation.

1. Introduction

The European Union's Critical Raw Materials list identifies Platinum Group Metals (PGM) - platinum, palladium, rhodium, osmium, iridium, and ruthenium - as materials facing a significant risk of supply scarcity. Automotive catalytic converters (ACC), are the most relevant application of PGM and correspond of more than 60 % of the market share.[1] ACC are employed to mitigate the environmental and health impacts of vehicle exhaust emissions, enabling modern vehicles to emit up to 100 times less harmful exhaust gases compared to those from the 1960s. [2,3] Among PGM, Pt, Pd, and Rh are particularly valuable in these applications for their high catalytic activity, resistance to

sulphur poisoning, thermal stability, and ability to facilitate key reactions, allowing for the development of efficient and compact catalysts.[2,4,5]

At their end-of-life, ACC turn into hazardous solid waste. Inadequately managed spent automotive catalytic converters (SACC) pose significant risks to human health and the environment due to the potential leaching of toxic metals.[6] Despite the rise of electric vehicles, internal combustion engine vehicles are expected to still dominate for decades, with projections suggesting that by 2040, only 500 million of 1.6 billion vehicles will be electric.[7] Consequently, SACC represent both a growing waste management challenge and a valuable secondary source of critical materials. Recycling SACC can significantly reduce the environmental impact of mining, conserving up to 95% of the energy required compared to primary extraction. For example, 1 kg of Pt can be recovered from approximately 2 tons of SACC, compared to 100 tons of mined ore.[5,6] Despite the criticality and value of PGM - averaging 30.74 €/g for Pt, 30.83 €/g for Pd and 149.50 €/g for Rh in 2024 [8] - current recycling rates from SACC remain below 50 %.[9] This indicates significant potential for improvement to secure sustainable PGM supply for existing and emerging technologies such as green hydrogen production and fuel cells.[10,11]

The recovery of PGM from SACC typically includes fundamental stages such as pretreatment, concentration, separation/purification, and final metal recovery. Conventional methods for recycling SACC and recovering PGM mainly rely on pyrometallurgical and hydrometallurgical concentration techniques. Pyrometallurgy involves processing metal sources at elevated temperatures, whereas hydrometallurgy involves the utilization of aqueous solutions to extract the metals.[12] Although pyrometallurgy has achieved technological maturity and exhibits high PGM recovery efficiency (~ 95 %), it continues to face challenges related to substantial capital investment, increased energy consumption, and low purity of PGM.[13] In contrast, hydrometallurgical techniques have gained considerable interest mostly due to their lower energy consumption compared to pyrometallurgy. However, their progress is hindered by technical limitations, including difficulties in achieving high extraction efficiencies, especially for Rh, due to the chemical inertness of PGM. To overcome this, halogenated compounds are widely used, as halogen ions can form stable soluble complexes with Pt, Rh, and Pd.[14] Additionally, leaching efficiency can be further enhanced by introducing a strong oxidizing agent. A common media for dissolution of PGM is *aqua regia*, a hazardous mixture of HCl and HNO_3 in a 3:1 volumetric ratio, where HCl forms water-soluble chlorocomplexes and HNO_3 acts as an oxidizing agent.[15,16] Leaching with *aqua regia* presents significant environmental and safety concerns due to its highly poisonous and corrosive nature, and the production of toxic gases and hazardous waste effluents.[17,18] Consequently, there is an ongoing search for alternative solvents that efficiently extract PGM from real matrixes while minimizing negative impacts on the environment and human health.

Possible replacements for *aqua regia* were proposed over the years for the extraction of PGM. The "organic *aqua regia*" for example, constituted by a mixture of thionyl chloride ($SOCl_2$) and organic solvents/reagents such as pyridine, can selectively leach Pd while Pt remains inert.[19] Systems using acetonitrile (CH_3CN) as a leaching agent were also proposed with oxidizing agents such as iron chloride ($FeCl_3$)[20] and H_2O_2[21] along with photocatalysis. [22] Another approach involves the improvement of *aqua regia* leaching. Hydrogen peroxide (H_2O_2) is a promising substitute for HNO_3, allowing high efficiency of PGM dissolution while lowering acid concentration and improving the leaching kinetics.[23–27] It is also advantageous to partially substitute HCl with another chloride ion supplier, such as the non-volatile chloride salts NaCl, [26,28]

NaClO, [25], $NaClO_3$, [29] $CuCl_2$ [26] and $AlCl_3$ [26,29,30] reaching efficiencies above 90 % for Pt and Pd leaching. Aluminium chloride ($AlCl_3$) stands out due to its ability to release three chloride ions per molecule, unlike many other chloride compounds. Additionally, the presence of aluminium ions tends to decrease the dissolution rate of the SACC substrate.[17]

Prominent results have also been obtained for leaching PGM with inorganic salts solutions. Particularly, NaCl was used as a leaching agent with the addition of ozone as oxidizing agent resulting in high efficiency for Pt (90 %) and Pd (80 %) in mild conditions (293 K).[31] Moreover, NaCl and $Al(NO_3)_3 \cdot 9H_2O$ can be used as leaching media, selectively and completely dissolving Pd.[18] On the other hand, Ding et al.[32] developed a microwave-assisted leaching with $AlCl_3$ solution that selectively recovered Pd and Pt from SACC. One of the most notable findings, reported by Forte et al.[33], demonstrated the use of 74 wt % hydrated $AlCl_3$ and $Al(NO_3)_3$ solutions, achieving extraction efficiencies of 64 % for Pt and 94 % for Pd at 80 °C for 4 h. In this system, the Al^{3+} ions act as strong Lewis acids, facilitating platinum dissolution whilst the presence of chloride complexes the dissolved platinum. The effective dissolution is attributed to the high acidity levels of concentrated solutions of salts containing high-valence metal ions, where the water-to-metal ion ratio is low enough to minimize outer-sphere hydration and the number of free water molecules.[34] The recovery of PGM was subsequently attempted through reductive precipitation using ascorbic acid, a process that was time-consuming (taking 3 days) and demonstrated low effectiveness, with a yield of only 25 %.

In this study, we aimed to develop a acid-free hydrometallurgical process for the recovery of PGM from SACC, offering an alternative to the traditional use of *aqua regia*. The approach is based on the use of aluminium-based salts for leaching, combined with pretreatment steps to enhance material accessibility and a selective recovery of Pt through anion exchange resins. Importantly, the work is structured to present a complete process, from pretreatment to leaching, selective separation, and preliminary scale-up, demonstrating the feasibility of a practical strategy for Pt recovery. This comprehensive methodology addresses the growing need for sustainable recycling technologies for critical raw materials.

2. Experimental

2.1. Materials

The $AlCl_3 \cdot 6H_2O$ (> 99 wt %) was acquired from Baker and Adamson. Hydrochloric acid (37 wt %) was purchased from Honeywell. Nitric acid (65 wt %) and $Al(NO_3)_3 \cdot 9H_2O$ (98.5 wt %) were acquired from Merck. Yttrium standard (995 $mg \cdot L^{-1}$ of Y(III) in 2 % nitric acid), poly(vinyl alcohol) (87-90 wt %) and Ambersep® 900 hydroxide form were purchased from Sigma-Aldrich. Thiourea (> 99 %) was acquired from Across Organics. SERVA was the supplier of silicone solution SERVA in isopropanol. All chemicals were used as received without further purification.

VALORCAR – Sociedade de Gestão de Veículos em Fim de Vida Lda, based in Lisbon, Portugal, generously supplied the SACC (reference: ITG189 C55 25162881). The catalyst was pretreated and subsequently analysed to identify the type and concentration of metals present. Although the specific origin of the SACC was not disclosed, the serial number confirmed that the catalyst originated from a diesel vehicle.

2.2. SACC pretreatment and characterization

VALORCAR provided the SACC already separated from the stainless-steel casing. The ceramic was initially broken down using a hammer. Afterwards, the structure was crushed using a Retsch Cross-Beater Mill SK1 with a 2 mm mesh. To further increase the surface area, the resulting powder was pulverized into finer particles using a Fritsch Pulverisette 23 ball mill equipped with a zirconium oxide chamber and balls, operating at a frequency of 40 s^{-1} for 5 min.

The analysis of the influence of different subsequent pretreatments was conducted, involving burning and washing the catalyst. During the burning process, the pulverized material was subjected to thermal treatment in a muffle furnace at 773 K for 6 h. The washing procedure was carried out by immersing the burned catalyst in distilled water for 6 h at 353 K and under constant agitation, followed by a vacuum-assisted filtration with 7-9 µm pore diameter filters (PRAT DUMAS) and drying the recovered powder in an oven at 323 K for 24 h. The resulting material was thoroughly blended to improve homogeneity and reduce potential inaccuracies in future analyses.

The characterization of the SACC was conducted using different analytical techniques. The solid in powder was analysed both by scanning electron microscopy with energy dispersive spectroscopy (SEM-EDS), conducted with a Bruker Nano GmbH microscope and X-ray diffraction (XRD), using a Bruker AXS instrument with Cu Kα radiation at 15 kV. The XRD diffractograms were analysed with the X'pert Highscore Plus software package, and the resulting patterns were compared to the International Centre for Diffraction Data (ICDD) database for identification.

The total metal composition was determined by analysing the liquid after leaching the catalyst powder in a 50 wt % *aqua regia* solution (HNO_3/HCl = 1:3 v/v) at 353 K for 6 h, under agitation at 350 rpm and a solid-to-liquid mass ratio of 1:10. To standardize the units for comparison based on the mass of catalyst used in the leaching process, m_c (g), and the leaching volume V_l (L), the metal concentration, C_{SACC} (mg.g^{-1} of SACC), was converted using equation (1):

$$C_{SACC\_AR} = \frac{C_{AR}.V_l}{m_c} \quad (1)$$

where C_{AR} (mg·L^{-1}) is the concentration of metals in the leachate, obtained through total reflection X-ray fluorescence (TXRF) analysis (see section 2.3 for more details).

2.3. Metal quantification

The quantification of metals was conducted using a TXRF spectrometer, specifically a Picofox S2 (Bruker Nano) equipped with a molybdenum X-ray source. The analysis was performed at a voltage of 50 kV and a current of 600 µA. Quartz glass carriers were pre-coated with 10 µL of a silicon in isopropanol solution (SERVA) and dried at 323 K. Samples were diluted in polyvinyl alcohol (1 wt %) and spiked with a known concentration of yttrium standard, adjusted according to the metal content of the samples. A 10 µL aliquot of this solution was transferred to a pretreated quartz carrier and subsequently dried at 353 K. The measurement time was 300 s.

The quantification of Pd and Rh is not feasible with TXRF due to peak overlap with Cl. Consequently, for the characterization, Pd and Rh were analysed using inductively coupled plasma-optical emission spectrometry (ICP-OES), specifically a iCAP 7400 (Thermo Scientific) equipped with a nebulizing system and employing optical emission spectroscopy for detection. The solutions were diluted to fall within the calibration curve

range (0.005–10 mg. L^{-1}) and were measured in triplicate. Al also could not be analysed using TXRF, and its concentration was therefore not monitored throughout the procedure.

2.4. Leaching optimization and analysis

To optimize the leaching process with aluminium salt mixtures, several experimental parameters were investigated, including the concentration of salts, the ratio of hydrated aluminium salts, the solid/liquid ratio, contact time, and temperature (see **Table 1**). The water content in each salt was measured using a Karl Fischer titrator (Metrohm – Eco KF Titrator) that confirmed the nominal water content. The leaching experiments were carried out in a vial heating block placed on a hot plate (Heidolph - MR Hei-Tec) with a rotation speed of 350 rpm. For experiments conducted at temperatures below room temperature, a thermostatic water bath was used. Following the leaching process, the residual SACC powder was separated by centrifugation at 10 000 rpm for 3 min, and the liquid phase was collected for metal analysis by TXRF. The different conditions tested are shown in **Table 1**.

Table 1. Conditions used in the optimization of parameters for the leaching with Al-based salts (columns correspond to a specific optimization step, while rows list the conditions used; variations in conditions for each step are in bold for clarity).

Conditions	**Optimization step**				
	[salts]	Cl/NO_3	S/L	T	T
Pretreatment	mill, burn	mill, burn	mill, burn, wash	mill, burn, wash	mill, burn, wash
[salts] (wt %)	**44, 35, 25, 15**	44	35	35	35
Cl/NO_3 (w/w)	1/1	**1/1, 1/0.4, 1/2.7**	1/1	1/1	1/1
S/L (w/w)	1/35	1/35	**1/5, 1/10, 1/20, 1/35, 1/50**	1/35	1/20
T (K)	353	353	353	**293, 313, 333, 353**	353
t (min)	360	360	360	360	**5, 15, 30, 60, 120, 180, 240, 300, 360**

To ensure accuracy and reliability, all experiments were conducted in duplicate. To compare with the results from *aqua regia* leaching, the units of the metal concentration, C_{SACC_Al} (mg.g^{-1} of SACC), were standardize using equation (2):

$$C_{SACC\_Al} = \frac{C_{Al}.V_l}{m_c} \quad (2)$$

where C_{Al} (mg·L^{-1}) is the concentration of metals in the leachate, obtained through TXRF analysis, m_c (g) is the mass of catalyst used in the leaching process and V_l (L) is the leaching volume.

In each case the leaching efficiency (*EE*%) was calculated in comparison with the *aqua regia* results according to the equation (3):

$$EE\ (\%) = \frac{C_{SACC\_Al}}{C_{SACC\_AR}} \cdot 100 \quad (3)$$

where C_{SACC_AR} and C_{SACC_Al} are the concentration of metal in mg.g^{-1} of treated SACC obtained, respectively, with *aqua regia* and Al-based salts mixtures leaching solutions. The final leaching solution obtained under optimized conditions was used to perform the separation analysis (section 2.5).

The redox potential of Al-based salts solution (35 wt %, $AlCl_3 \cdot 6H_2O$/ $Al(NO_3)_3 \cdot 9H_2O$ = 1 w/w), *aqua regia* (50 wt %, HCl / HNO_3 = 3 v/v), 6 M HCl and 1 M HCl + 3.8 M NaCl was measured at 298 K using a pHenomenal ORP 220 oxidation-reduction sensor connected to a pHenomenal® pH/mV/°C bench meter model pH 1100L (VWR). The sensor uses an Ag/AgCl reference electrode system with an offset of 207 mV at 298 K relative to the standard hydrogen electrode. All reported results incorporate this offset to enable direct comparison with standard hydrogen potentials from the literature.

2.5. Anionic exchange resin separation

Ambersep® 900 OH-form was activated by titration with 0.1 M HNO_3 until neutral pH (~7) was achieved. This process took place at room temperature (~298 K) under constant agitation in an orbital mixer set to 240 rpm. Following titration, all acid was removed, and the activated resin was washed with distilled water for 1 h. Finally, the water was removed, and the resin was dried in an oven at 303 K for 24 h before storage.

To evaluate Pt separation using Ambersep® 900, all mixtures were subjected to constant vertical rotation using an IKA TRAYSTER digital rotator at room temperature. The optimization of the resin-to-liquid (R/L) ratio was carried out by testing ratios of 1/50 w/w, 1/100 w/w, and 1/200 w/w, with a rotation of 80 rpm for 2 h with a mixture of the activated resin and the solution obtained after leaching under the optimized conditions. After 2 h, the leachate was collected, and the metal content was quantified by TXRF. The resin sorption ratio (q) was calculated using equation (4).

$$q = \frac{V_r \cdot (C_{Al} - C_r)}{m_r} \quad (4)$$

where V_r (L) represents the volume of the leachate in contact with the resin, C_r(mg·L^{-1}) denotes the metal concentration after the leachate contacted the resin and C_{Al} (mg·L^{-1}) indicates the metal concentration before the leachate contacted the resin, m_r (g) refers to the mass of the resin. The resin extraction efficiency percentage (EE_r %) was calculated using equation (5):

$$EE_r(\%) = \frac{C_{Al} - C_r}{C_{Al}} \cdot 100 \quad (5)$$

Resin isotherms assays were conducted employing 35 wt % aluminum salts solutions ($AlCl_3 \cdot 6H_2O$/ $Al(NO_3)_3 \cdot 9H_2O$ = 1 w/w) with a known Pt concentration for 2 h on activated Ambersep 900® with R/L of 1/100 w/w and rotation of 80 rpm. The solution was collected, and the metal content was quantified by TXRF. The sorption data obtained was then fitted to two well-established models, namely the Langmuir, equation (6), and Freundlich, equation (7).[35]

$$q_e = q_{max}\left(\frac{K_L \cdot C_e}{1 + K_L \cdot C_e}\right) \quad (6)$$

$$q_e = K_F \cdot C_e^{1/n} \quad (7)$$

where q_{max} (mg·g^{-1}) is the adsorbent maximum sorption capacity, C_e (mg.L^{-1}) is the adsorbate concentration in the solution at equilibrium, q_e (mg.g^{-1}) is the resin sorption ratio (Equation 4) at equilibrium, K_L (g·mg^{-1}) is the Langmuir constant, and K_F (L$^{1/n}$·mg$^{(1-1/n)}$·g^{-1}) and n (dimensionless) are the Freundlich constants.

The adsorption kinetic was assessed. Six different contact times were evaluated: 15 min, 30 min, 60 min, 120 min, 240 min, and 300 min. These experiments were performed with a 1/100 R/L ratio (w/w), under constant agitation of 240 rpm in an orbital mixer. The metal content was quantified by TXRF after the separation of the resin and the leachate by centrifugation (10000 rpm, 3 min).

2.6. Pt elution

Following the Pt sorption, the resin was washed with distilled water at room temperature under constant vertical agitation (80 rpm) for 1 h. Pt stripping was evaluated by using thiourea solutions at different concentrations: 0.1 M, 0.2 M, 0.5 M, and 1.0 M. Each thiourea solution was tested on the washed resin at a R/L ratio of 1/100 w/w. The mixture was then subjected to constant vertical rotation at 80 rpm for 2 h at room temperature. The thiourea solution was collected, and the metal content was quantified by TXRF.

2.7. Scale-up

In the scalability assessment, distinct methodological adjustments were necessary to accommodate the increased volume of leaching solution from 2 mL in prior experiments to 120 mL in this process. The leaching procedure was conducted in a borosilicate narrow-neck vial, which was immersed in a paraffin-heated bath to maintain a stable temperature. For mixing, an overhead stirrer (Hei-TORQUE, Heidolph Instruments) was employed at a constant speed of 550 rpm, with agitation maintained for up to 24 h. The obtained mixture was then filtrated using vacuum-assisted filtration to separate the liquid and solid phases. The liquid phase was then reused for up to five cycles with the addition of new SACC powder for each cycle and the metal concentration was quantified by TXRF. The extraction efficiency for cycle 1 was calculated using equation (3) and for the following cycles (EE_n, where n = 2, 3, 4, 5) was calculated as shown in equation (8):

$$EE_n\,(\%) = \frac{(C_{Al,\,n} - C_{Al,\,(n-1)}) \cdot V_{l,\,n}}{m_{c,\,n}} \cdot \frac{100}{C_{SACC\_AR}} \quad (8)$$

where $C_{Al,n}$ (mg·L^{-1}) is the concentration of metals in the leachate, obtained through TXRF analysis, $V_{l,n}$ (L) is the initial volume of leachate and $m_{c,n}$ (g) the mass of SACC used in each n cycle.

For the adsorption with Ambersep® 900, a new kinetics study was performed with the concentrated leachate solution. The conditions included a R/L of 1/100 w/w for up to 24 h at a constant vertical rotation of 80 rpm at room temperature. This step was followed by a filtration to separate the resin that was washed with water for 1 h. The next step was the analysis of the concentration for the stripping with thiourea.

3. Results

3.1. SACC characterization and pretreatment

The SACC was physically and chemically characterized, with a focus on the influence of different pretreatments on metals concentration and leaching efficiency. The milling process was employed to reduce the size of catalyst particles, thereby increasing their accessible surface area. In contrast, the burning treatment aimed to eliminate impurities, such as accumulated oils, which can negatively affect the leaching process.[17] The morphology of the powder was analysed using SEM-EDS, which provided detailed information regarding the composition of the catalyst before and after burn (**Figure 1** and **Table S1**).

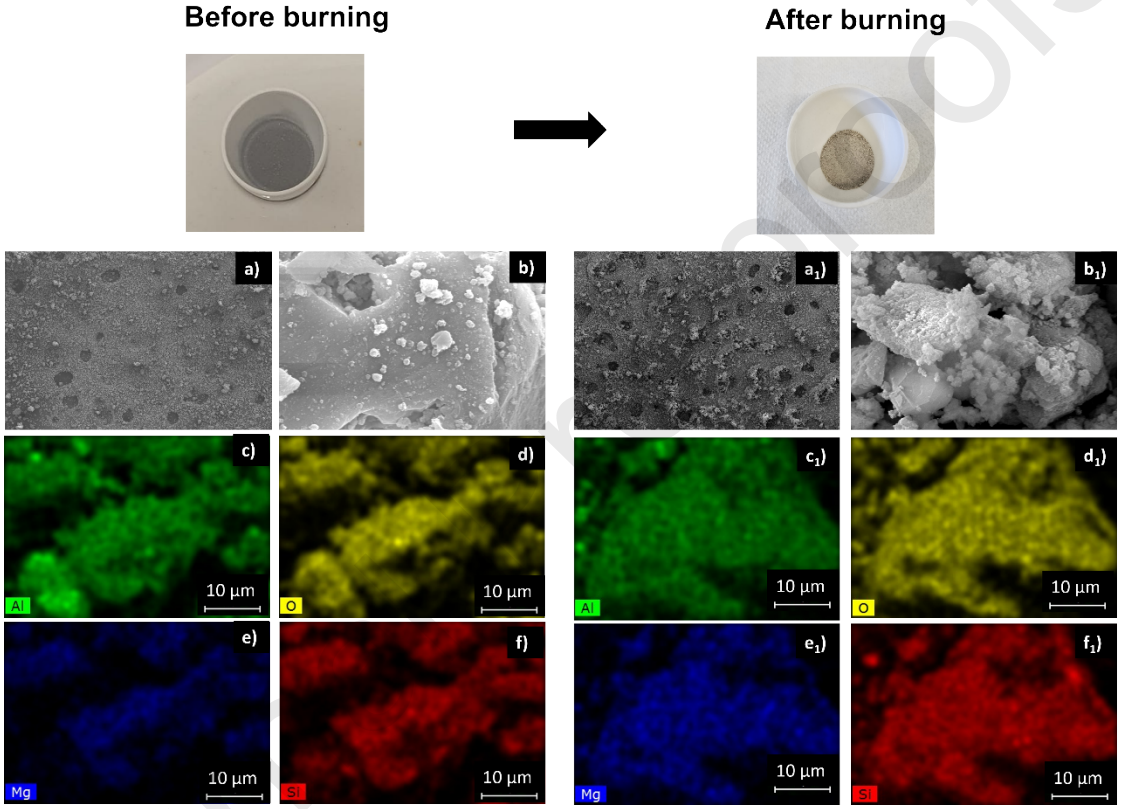

Figure 1. Macroscopic and SEM-EDS images of SACC powder before and after the burning process. Top images: macroscopic photographs showing the material before (left) and after (right) burning. SEM images (a, a1) and (b, b1) correspond to magnifications of 40 and 10000 times, respectively; SEM-EDS elemental mapping images show the distributions for Al (c, c1), O (d, d1), Mg (e, e1), and Si (f, f1).

As shown in **Figure 1**, the SACC exhibited a coarse surface, which is attributed to the washcoat. This coarse surface facilitates the distribution of PGM, enhancing the interaction with the exhaust gases. The removal of impurities through the burning process is clearly demonstrated by the colour change in the catalysts, shifting from dark grey to light brown, probably due to the elimination of hydrocarbon residues. The overall morphology of the catalyst was slightly affected by the burning process, resulting in a more segmented appearance. The presence of oxygen was expected, as this element is essential for the catalytic activity of SACC in gas oxidation and reduction processes. Furthermore, the continuous exposure of the catalyst to high temperatures (> 673 K)

accounts for the oxygen accumulation and the presence of sulphur from combustion products.

SACC chemical characterization was conducted using XRD, TXRF and ICP. The XRD analysis offers a comprehensive understanding of the SACC crystalline structure (**Figure 2**), identifying cordierite ($Mg_2(Al_4Si_5O_{18})$) as the predominant phase. This result is in accordance with the high presence of Al, O, Mg and Si indicated in SEM-EDS analysis (**Table S1**). The comparison between the milled and milled-and-burned samples in **Figure 2** shows that each peak aligns precisely, indicating that the burning process did not alter the structure of cordierite but solely removed the hydrocarbon residues.

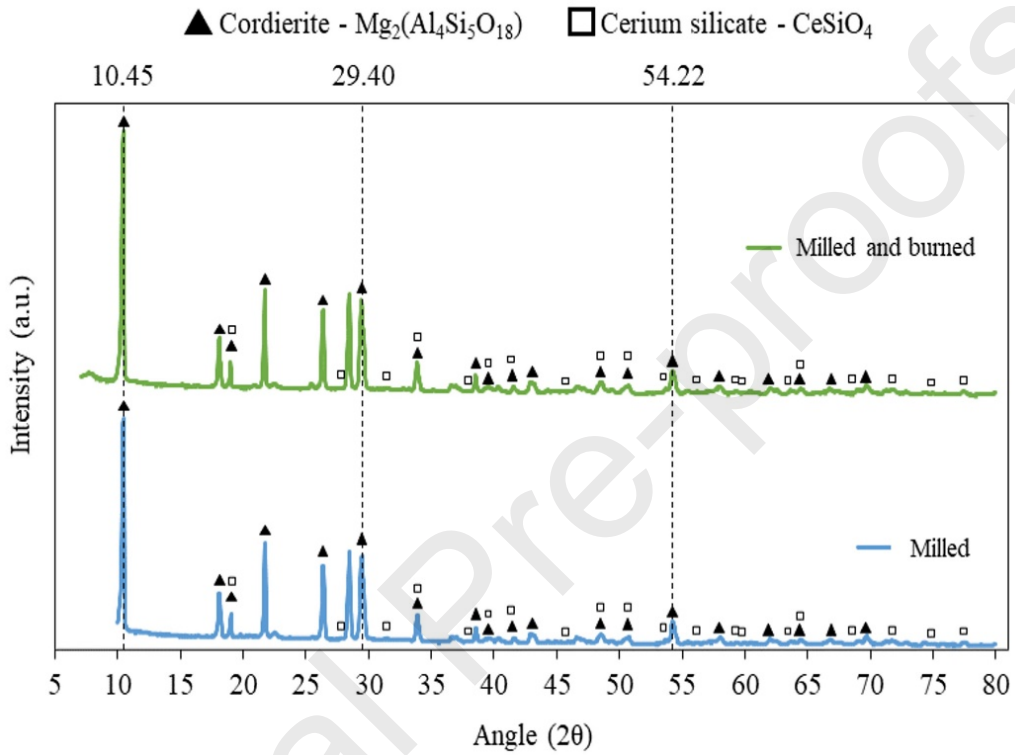

Figure 2. XRD analysis of SACC powder before and after burning process.

Although XRD analysis revealed a significant concentration of cerium silicate ($CeSiO_4$), SEM-EDS did not detect the presence of cerium. The detection of cerium silicate was anticipated due to its well-established role in enhancing CO oxidation and hydrocarbon conversion via its oxygen storage capacity (OSC).[36] The observed discrepancy between the two analytical techniques may be attributed to the limitations of SEM-EDS, which analyses only a small portion of the sample and performs spot analysis, potentially resulting in an incomplete representation of the overall sample composition.

Leaching with *aqua regia* was performed as a reference method to establish a baseline for comparison, both in terms of the chemical composition of the SACC powder and the effects of different pretreatment procedures on the washcoat. The results are presented in **Figure 3**. Notably, the removal of impurities through burning increased the concentration of metals per gram of catalyst. The wash of the SACC powder with water after the burning process was found to effectively eliminate metals such as Ni (40 %), Zn (80 %) and Ce (97 %). The resultant solution, which is predominantly rich in Ce (**Table S2**), presents a valuable opportunity for this metal recovery. As a light rare earth element, Ce is of particular importance due to its criticality and high value, as highlighted in the European Union's Critical Raw Materials list.

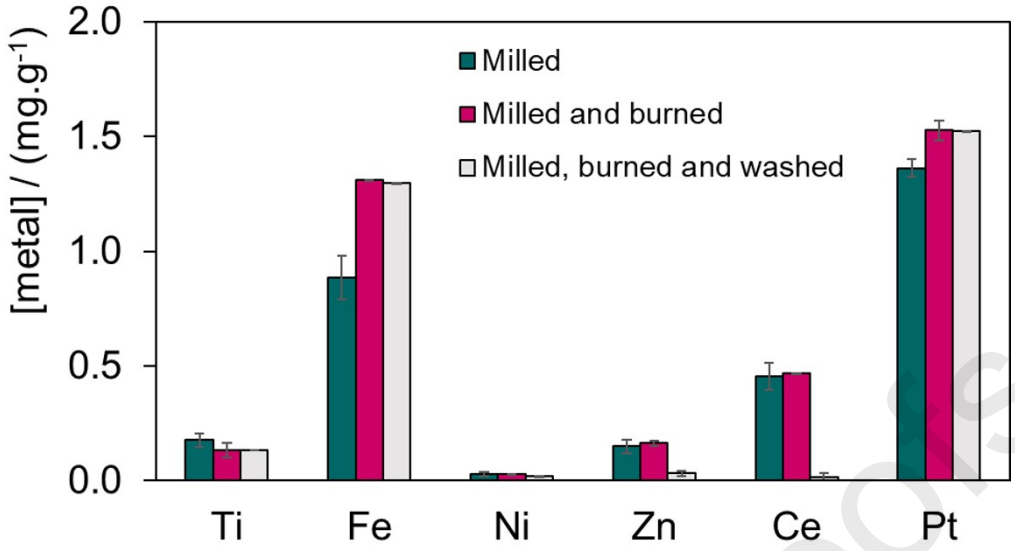

Figure 3. The effect of SACC pretreatment on final metal concentration (*aqua regia* leaching, S/L ratio = 1/10 w/w, T = 363 K, 350 rpm, t = 6 h).

ICP-OES analysis revealed that Pd and Rh are absent or at least below the detection limit of the equipment (0.005 $mg.kg^{-1}$) in the treated SACC. The absence of Rh is consistent with expectations, as Rh is not typically found in diesel engine vehicles that are most of the times made by Pt and/or Pd. [37,38]. Other studies have also reported Pt as the only detectable PGM in diesel catalysts, particularly in older vehicles, while Pd and Rh are present in only trace amounts, if at all, even when using aggressive leaching agents such as HF and $HClO_4$.[38–40] As Pt is the only PGM present in the real catalyst sample, this study is focused to optimizing Pt extraction.

3.2. Leaching

3.2.1. Alternative leaching media

Aqua regia is the traditional media for PGM leaching and despite its effectiveness, its highly corrosive nature raises health, safety, and environmental concerns. To mitigate these risks, less harmful leaching alternative media have been tested for the extraction of metals from SACC, such as 6 M HCl, a mixture of 1 M HCl and 3.8 M NaCl, and a mixture of hydrated $AlCl_3$ and $Al(NO_3)_3$.[14,33] As shown in **Figure 4**, the 6 M HCl solution was the most effective leaching medium for dissolving Ti, Fe, Ni, and Ce. In contrast, the HCl and NaCl mixture demonstrated the lowest efficiency across all elements. This difference may be attributed to the harsher environment created by concentrated HCl, which, due to potential chlorine formation and its higher oxidizing capability, enhanced metal extraction compared to the HCl-NaCl mixture. The mixture of Al-based salts proved to be more effective in dissolving Pt than the other leaching media tested, due to the presence of nitrate, which increased the solution's oxidizing power and improved the dissolution of precious metals. Furthermore, Al-based salts mixture showed marked selectivity for Pt dissolution, offering potential benefits for Pt purification.

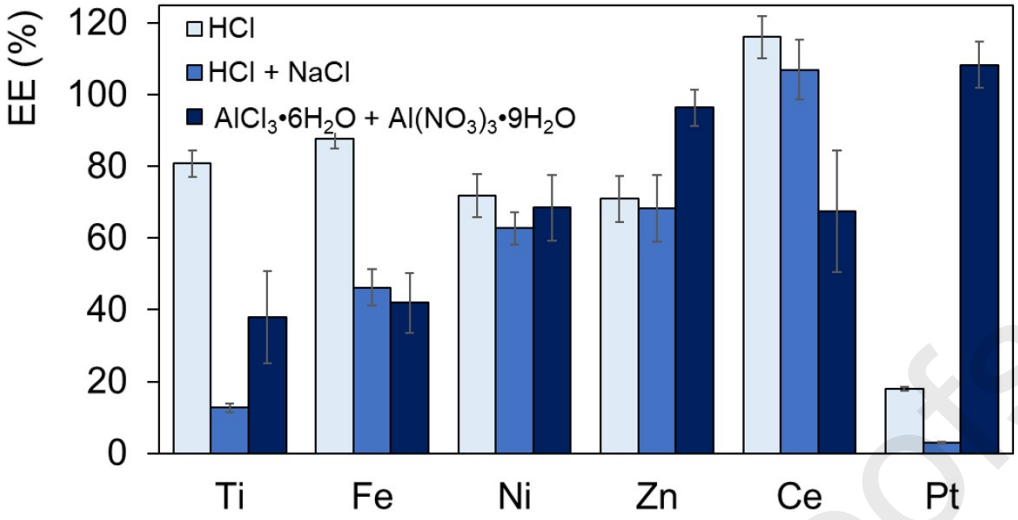

Figure 4. Leaching extraction efficiency for different tested leaching media on milled SACC. Experimental details are presented in the Supplementary Material (**Table S3**).

An efficient extraction process is closely related to the oxidation–reduction potential of the leaching solution. In chloride media, Pt predominantly exists in the chloro-complex form $[PtCl_6]^{2-}$. Enhanced leaching efficiency can be achieved by introducing an oxidizing agent, as indicated by the electrode potential shown in equation (9).[41]

$$Pt + 6Cl^- \leftrightarrow PtCl_6^{2-} + 4e^- \qquad E^0 = -740\ mV \tag{9}$$

Therefore, an oxidizing medium with a potential greater than 740 mV is necessary to form the chloride complex. In the case of *aqua regia*, nitric acid acts as a suitable oxidizing agent with a standard oxidation potential of 960 mV. For instance, the final solution of *aqua regia,* used for characterization (50 wt % , HCl/HNO_3 = 3/1 v/v), reaches an oxidation–reduction potential of (1167.9 ± 0.1) mV. In comparison, the solution of aluminium salts with a concentration of 35 wt % possesses a potential of (822.2 ± 0.3) mV, which is sufficient to promote the leaching process. The redox potential of the other media tested were also measured. The results were (668.8 ± 0.1) mV for 6M HCl and (728.8 ± 0.1) mV for the mixture of HCl and NaCl, justifying the lower extraction of Pt in these solutions.

Given its superior sustainability, efficiency, and selectivity, the hydrated Al-based salts mixture was selected as the leaching medium for optimizing Pt recovery from the SACC powder. Previous studies have demonstrated that, in highly concentrated aluminium salt solutions, the dominant oxidative mechanism for PGM dissolution is not the direct oxidation by nitrate ions, as in *aqua regia*, but rather the generation of highly reactive hydroxyl radicals including hydroxyl (•OH) and oxygen ($•O_2^-$) species through proton dissociation processes and photovoltaic effect.[18,32]

The leaching mechanism thus relies on the oxidation of metallic Pt to soluble Pt(IV) species, followed by complexation with chloride ions to form stable $[PtCl_6]^{2-}$ complexes under strongly acidic conditions. At higher pH values, these complexes may hydrolyze, forming hydroxy complexes that are less stable and could limit extraction efficiency.

Therefore, maintaining a low pH environment during leaching is essential to ensure the effective formation and stabilization of $[PtCl_6]^{2-}$ and to maximize Pt recovery. [33]

This mechanism avoids the formation of significant amounts of NO_x gases, which would otherwise be expected if nitrate ions were directly acting as oxidizing agents. In our experiments, no darkening of the solution was observed during the leaching cycles, and the extraction efficiency remained stable over multiple reuse cycles (as demonstrated further), supporting the environmental sustainability of the process. Furthermore, the use of aluminium chloride instead of free hydrochloric acid has been reported to reduce the volume of released gases by approximately 60%.[30] In addition, the aluminium salts employed are solid, non-volatile compounds that are relatively safe to handle compared to concentrated mineral acids, thus minimizing occupational hazards during operation.

3.2.2. Leaching optimization

In this study the leaching process with a mixture of hydrated $AlCl_3$ and $Al(NO_3)_3$ was optimized to achieve the highest Pt extraction. The optimized parameters were the total concentration of salts in water, the mass ratio between aluminium chloride and aluminium nitrate (Cl/NO_3), the solid-to-liquid ratio (S/L), temperature (T) and contact time (t).

An initial assay was conducted to evaluate the effect of salt concentrations on leaching efficiency. A solution containing 74 wt % salts was previously reported for the leaching of Pt.[33] However, experimental challenges arose during the handling of the leachate at room temperature due to the limited solubility of aluminum chloride. To address this limitation, subsequent analyses were performed under conditions ensuring that all salt combinations remained below their solubility limits at room temperature (298 K) while maintaining extraction efficiency. The results obtained are illustrated in **Figure 5**. Notably, Pt extraction efficiencies remained comparable at salts concentrations of 44 wt % and 35 wt %, with extraction rates of (91 ± 7) % and (94.1 ± 0.4) %, respectively. Reducing the salt content from 35 wt % to 15 wt %, however, resulted in a decline in Pt extraction efficiency to ~30 %.

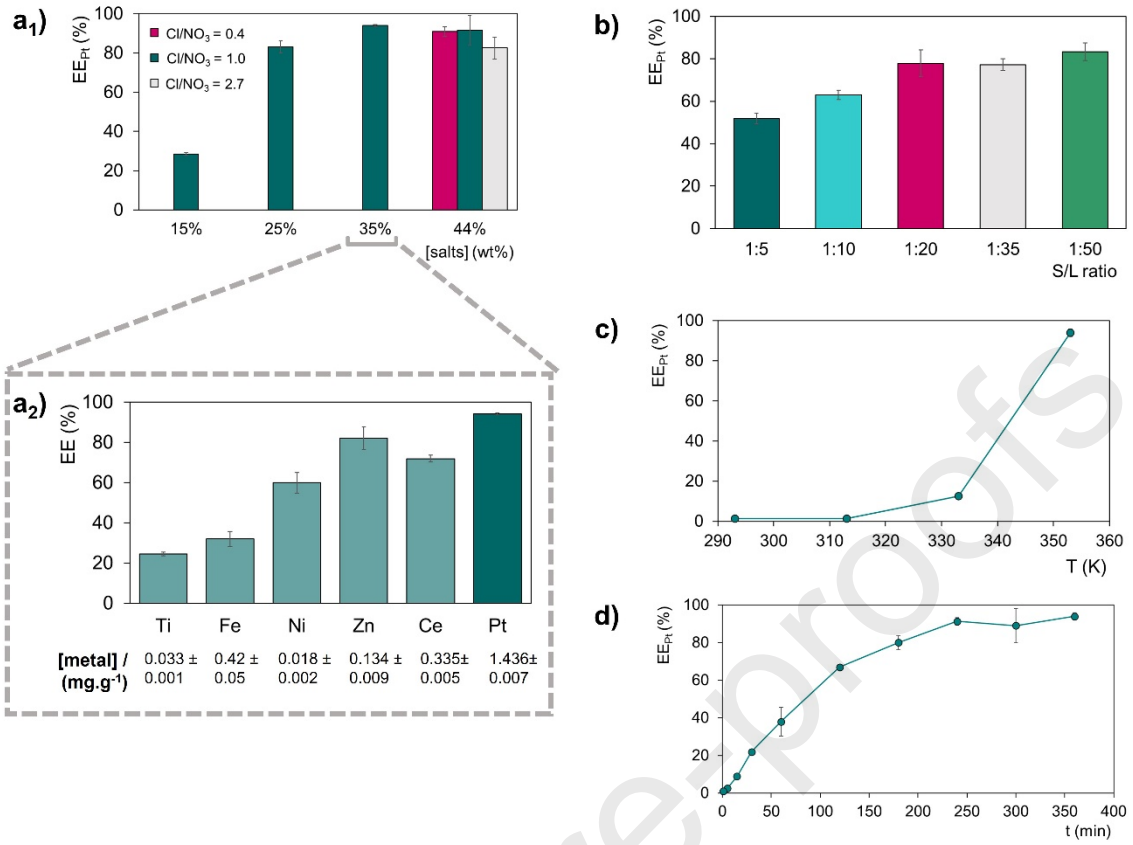

Figure 5. Optimization of leaching conditions using Al-based salts mixtures for the efficient dissolution of Pt from SACC pretreated powder: (a_1/a_2) salts concentration and $AlCl_3 \cdot 6H_2O/Al(NO_3)_3 \cdot 9H_2O$ (Cl/NO_3) mass ratio effect; (b) solid-to-liquid ratio effect; c) temperature effect; (d) contact time. The experimental conditions used in each parameter optimization are reported in **Table 1**.

Regarding the ratio between salts, increasing the concentration of $Al(NO_3)_3 \cdot 9H_2O$ has no significant impact, while its decrease leads to a slight drop in Pt extraction, possibly due to a reduction in the mixture's oxidizing capability (**Figure 5a$_1$**). Considering all factors, the optimal leaching conditions were determined to be a salt concentration of 35 wt % and a $Cl:NO_3$ ratio of 1 allowing (94.1 ± 0.4) % of Pt extraction. Notably, the final Cl to NO_3 ratio is lower than 3:1 commonly found in *aqua regia* acid solutions. Furthermore, when evaluating the extraction of the remaining metals with a 35 wt % salts solution (**Figure 5a$_2$**) it is evident that the leaching process is less effective for Fe, which is the primary contaminant in *aqua regia* leaching (**Figure 3**). Consequently, this process demonstrates increased selectivity for Pt. For the remaining concentrations, the results can be seen in **Figure S1** and **Figure S2**. Overall, the obtained results are remarkable and better than those reported by Forte et al.,[33] who used a higher salt concentration (74 wt %) while achieving a leaching efficiency of just 60 % for Pt. However, it is important to stress that comparisons must be made with caution in situation when real matrixes are used, because they are inherently different and may impact the results.

A decrease in the solid-liquid ratio was found to enhance Pt leaching efficiency (**Figure 5b**). This improvement is attributed to the increased mass transfer achieved by increasing the leachate volume for the same amount of sample. Similar outcomes for Pt extraction were observed across solid-liquid ratios ranging from 1/20 to 1/50. Consequently, a solid-liquid ratio of 1/20 (w/w) was selected as the optimal condition to

minimize the required volume of leaching solution, thereby reducing the associated process costs. For other metals, the result can be seen in **Figure S3**.

The effect of contact time and temperature on the leaching process was also evaluated. Pt dissolution rate exhibits a notable susceptibility to temperature variations, as showed in **Figure 5c**, escalating markedly from (1.4 ± 0.1) % at 293 K to (94 ± 2) % at 353 K. Temperatures beyond 353 K were not explored due to the substantial water loss during the leaching procedure. At 353 K, equilibrium is achieved at 240 min (**Figure 5d**), meaning that most of Pt within the matrix was leached, resulting in a leaching efficiency of (91 ± 2) %. The behaviour for other metals can be seen in **Figure S4**. Overall, the optimal leaching conditions are achieved when the milled, burned and washed catalyst is leached with a 35 wt % aqueous solution of $AlCl_3 \cdot 6H_2O$ + $Al(NO_3)_3 \cdot 9H_2O$ (1/1), at a solid-to-liquid ratio 1/20 w/w, 353 K for 240 min. The composition of the leachate obtained under optimal conditions is presented in **Table 2**.

Table 2. Metal composition of the leachate obtained after leaching pretreated SACC powder with Al-based salts solution at optimized conditions. ([salts]=35 wt %, Cl/NO_3 = 1 w/w, S/L ratio = 1/20 w/w, T = 363 K, t = 4 h).

Element	Composition / ($mg \cdot L^{-1}$)	STD / ($mg \cdot L^{-1}$)
Ti	1.48	0.08
Fe	17.54	0.35
Ni	0.82	0.05
Zn	1.18	0.12
Ce	5.23	0.58
Pt	86.05	1.33

3.2.3. Mechanism of Pt extraction

To better understand the leaching mechanism involved in Pt extraction, the shrinking core kinetic model was applied and adjusted to describe the process. In the shrinking core model, it is assumed that an intermediate layer forms between the unreacted core and the leaching medium. As leaching progresses, the unreacted core shrinks towards the centre of the particle, causing a decrease in the particle's radius. Different linear adjustments can be used, based on the rate-limiting step in the dissolution process: the layer mass transfer control model, equation (10), the surface chemical reaction model, equation (11), and the residual layer diffusion model, equation (12).[42,43]

$$x = k_1 t \quad (10)$$

$$1 - (1 - x)^{\frac{1}{3}} = k_2 t \quad (11)$$

$$1 - 3 \cdot (1 - x)^{\frac{2}{3}} + 2 \cdot (1 - x) = k_3 t \quad (12)$$

where x is the molar fraction reacted, k_1, k_2 and k_3 are the fitting line slopes, and t is the leaching time (min).

The kinetic data were fitted to the shrinking core linear models assuming no initial extraction (t = 0, x = 0) (**Figure S5**). For temperatures of 333 K, 313 K and 293 K the adjustment was based on the leaching efficiencies obtained up to 480 min. For the temperature of 353 K, the parameters were estimated using the leaching efficiencies obtained up to 240 min, before the leaching efficiency plateau was reached. The constant values and correlation coefficients obtained for each model are reported in **Table 3**.

Table 3. Experimental shrinking core model constants values and their respective correlation coefficients.

	Layer mass transfer		**Surface chemical reaction**		**Residual layer diffusion**	
T / (K)	**k_1 / $(min)^{-1}$**	**R^2**	**k_2 / $(min)^{-1}$**	**R^2**	**k_3 / $(min)^{-1}$**	**R^2**
353	4.35×10^{-3}	0.971	2.36×10^{-3}	0.998	2.18×10^{-3}	0.974
333	3.60×10^{-4}	0.981	1.26×10^{-4}	0.977	2.00×10^{-5}	0.794
313	3.42×10^{-5}	0.762	1.14×10^{-5}	0.763	1.50×10^{-7}	0.882
293	4.34×10^{-5}	0.652	1.45×10^{-5}	0.662	1.88×10^{-7}	0.586

The surface chemical reaction control model demonstrated the best fit to the experimental data at 353 K, the optimal temperature, with a correlation coefficient of 0.998. This suggests that the leaching process is primarily governed by chemical reactions occurring on the catalyst surface. The fact that chemical reactions are generally more sensitive to temperature changes compared to diffusion processes [44] explains the results observed in the temperature optimization study. The surface chemical reaction model also provides a reasonable fit to the results at temperatures of 353 K and 313 K, but the results at 293 K exhibit a poor fit across all models considered due to very low leaching efficiencies at this temperature.

Another important parameter to understand the leaching process is the activation energy (E_a), estimated by the empirical Arrhenius law, equation (13):

$$ln\, k = ln\, A - \frac{E_a}{RT} \quad (13)$$

where k is the leaching constant rate (min^{-1}) of the best fitted shrinking core model, A is the Arrhenius constant (min^{-1}), and E_a is the activation energy ($J{\cdot}mol^{-1}$). The detailed process used to calculate the E_a is provided in the Supplementary Material (**Figure S6**). The leaching rate constant for 293 K was excluded from the linearization due to its outlier behavior. The estimated E_a was found to be (122 ± 11) $kJ.mol^{-1}$. Since E_a values above

40 kJ.mol^{-1} are typically indicative of chemically controlled reactions, this reinforces our interpretation that the surface chemical reaction is controlling the leaching process.[44]

3.3. Pt purification

3.3.1. Adsorption by anionic exchange resin

Pt selective separation was performed using an activated anionic exchange resin, the Ambersep® 900 in the OH-form, by contacting it with the aluminum salts leachate. This activation involved titrating the resin with 0.1 M HNO_3 until neutral pH was achieved, followed by a water rinse. The activation serves two purposes: to prevent metal precipitation caused by the alkaline pH of the resin and to align the anion of the resin with aluminum nitrate present in the leaching solution. This alignment minimizes any potential changes in the leachate composition and facilitates its reuse.

Ambersep® 900 OH is a strong base anion exchange resin composed of a styrene-divinylbenzene copolymer matrix functionalized with quaternary ammonium groups, as illustrated in **Figure S7**. Its high affinity for negatively charged platinum complexes, such as $[PtCl_6]^{2-}$, is attributed to anion exchange mechanisms governed by the Hofmeister series. In this context, the lower charge density and higher polarizability of the platinum complex compared to the nitrate ion on the resin promote efficient exchange and subsequent adsorption of Pt onto the resin surface. [45,46]

This resin shares structural and functional characteristics with other strong base anion exchange resins, such as the Amberlite, Amberjet and Dowex series, which have been successfully applied for PGM recovery in previous studies. [47–49] These resins are based on similar styrene-divinylbenzene copolymer matrices and possess quaternary ammonium functional groups, providing high anion exchange capacities and hydrophilic properties that promote the adsorption of polar metal complexes. Given these similarities, Ambersep® 900 OH was selected as a suitable candidate for the selective recovery of platinum.

To evaluate the sorption efficiency and determine the impact of the resin-to-liquid (R/L) ratio, three different R/L ratios were examined: 1/50, 1/100, and 1/200 w/w in contact with the leaching solution referred in **Table *2***. The results obtained for the metal extraction rate, EE_r (equation 5) and metal sorption ratio, q, (equation 4) are presented in **Figure 6**. The results reveal a selective recovery of Pt at all R/L ratios. Moreover, as the R/L ratio decreases, the EE_r decreases while q increases. The results indicate that as the mass of resin increases, the amount of Pt adsorbed also increases, with no observed plateau. This suggests that the system is operating below the resin's maximum adsorption capacity. However, at the highest resin amount (1/50), the lowest Pt sorption ratio is observed. Additionally, the difference in extraction rates between the R/L ratios of 1/50 (94 %) and 1/100 (87 %) is relatively small. Thus, an optimal balance between EE_r and q is achieved at an R/L ratio of 1/100, which is considered the ideal ratio.

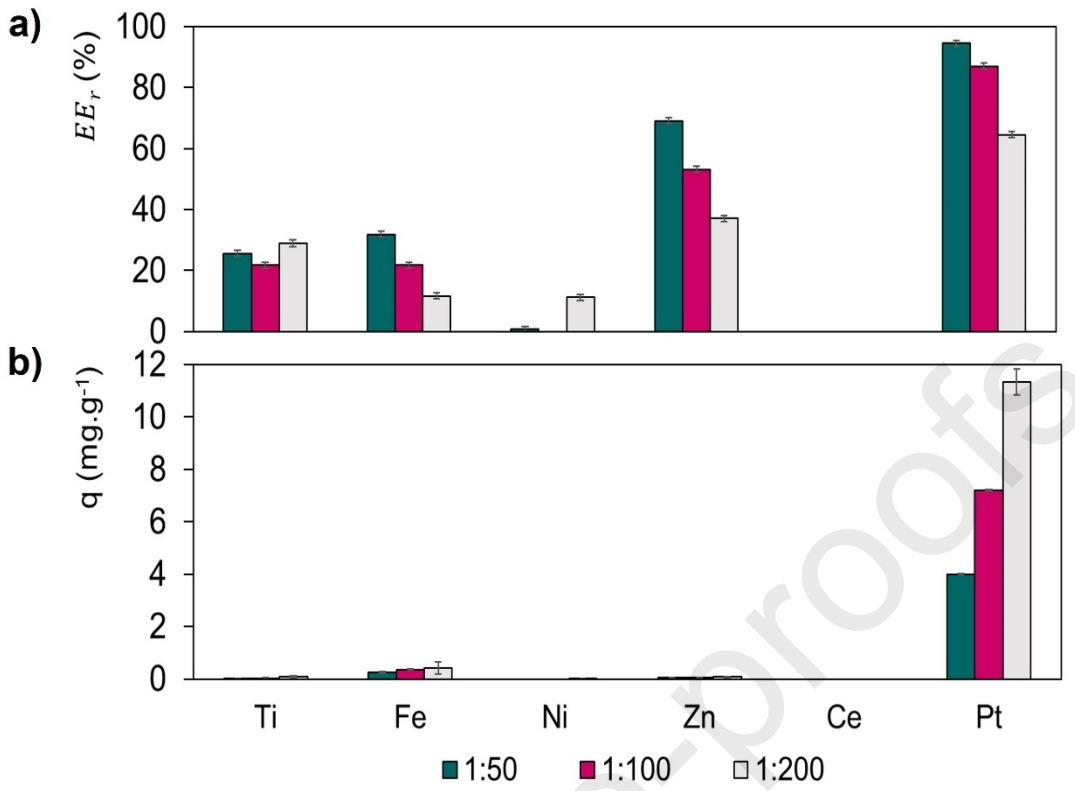

Figure 6. Analysis of the influence of the R/L ratio on (a) metals extraction rate from the aluminum salts solution by Ambersep® 900 (EE_r), and (b) metals sorption ratio (q) on Ambersep® 900 (room temperature, t = 2 h, 80 rpm, vertical rotation).

3.3.2. Adsorption isotherms

Adsorption isotherms were measured to determine the theoretical loading capacity and to ascertain whether platinum sorption onto the resin occurs via a monolayer or multilayer process. The resulting sorption data were then fitted to two well-established models: the Langmuir model (equation 6) and the Freundlich model (equation 7). Both models were fitted to the experimental data, as shown in **Figure 7**.

a)

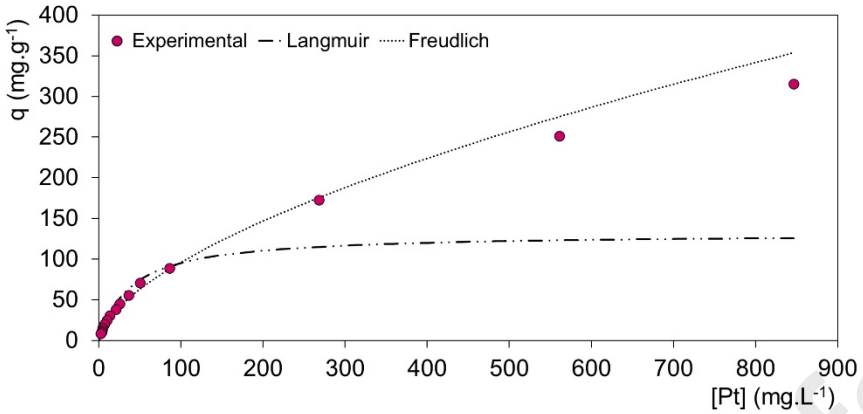

b)

Langmuir				Freundlich		
q_{max} (mg·g^{-1})	K_L (g·mg^{-1})	R^2	ΔG^0 (kJ.mol^{-1})	K_f (L$^{1/n}$·m$^{(1-1/n)}$g^{-1})	n	R^2
134.58	0.03	0.989	-3.97	5.80	1.64	0.991

Figure 7. Sorption isotherms of Pt onto Ambersep® 900 at 25 ºC and corresponding fit of Langmuir and Freundlich models: a) plotted data, with experimental data represented by dots and fitted models by lines; b) parameters of isotherm models.

The Freundlich model demonstrates a superior fit to the obtained data, indicating that Pt sorption occurs in multilayer on heterogeneous sites and interactions exist between adsorbates. The Langmuir model also shows a reasonable description of the experimental data at low concentrations; however, it is evident that model fails to accurately represent the system at high Pt concentration since no plateau is reached. These results are complementary to what was experimentally observed in the analysis of R/L ratio effect (**Figure 6**) since the saturation of the resin was never observed.

3.3.3. Resin adsorption kinetics

The Pt sorption kinetics was evaluated by fitting two different models: the Lagergren's pseudo-first order model (PFO), equation (14), and Ho's pseudo-second order model (PSO), equation (15):[50,51]

$$q_t = q_e(1 - e^{-k_1 t}) \quad (14)$$

$$q_t = \frac{q_e^2 k_2 t}{1 + q_e k_2 t} \quad (15)$$

where q_t (mg·g^{-1}) is the sorption capacity of activated Ambersep® 900 at each time, q_e (mg·g^{-1}) is the sorption capacity at equilibrium and k_1 (min^{-1}) and k_2 (g·mg^{-1}·h^{-1}) are the rate constants of PFO and PSO models, respectively. The results are presented in **Figure 8**. The Pt sorption process reaches a plateau at 120 min, representing 90 % of the total metal amount adsorbed onto the resin (**Figure S8**). This high selectivity is advantageous, as maintaining the high purity of Pt is essential for its commercial value. Ho's kinetic model (PSO) demonstrates a better fit compared to Lagergren's model (PFO). This second-order mechanism presumes that chemisorption is the rate-limiting step, with

sorption activity attributed to valence forces involving electron sharing or exchange between the metals and the resin.[52]

a)

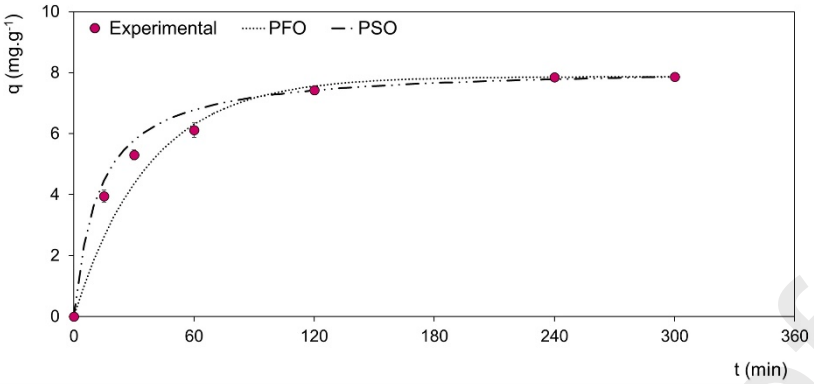

b)

Lagergren's (PFO)			Ho's (PSO)			Experimental value
k_1 (min^{-1})	q_e ($mg \cdot g^{-1}$)	R^2	k_2 ($g \cdot mg^{-1} \cdot h^{-1}$)	q_e ($mg \cdot g^{-1}$)	R^2	q_e ($mg \cdot g^{-1}$)
0.026	7.146	0.990	0.010	8.190	0.997	7.868

Figure 8. Kinetic study of Pt adsorption onto Ambersep® 900 at room temperature and corresponding fit of the Lagergren's (PFO) and Ho's (PSO) models. a) plotted data, with experimental data represented by dots and fitted models by lines; b) parameters of kinetic models.

3.3.4. Selective elution of Pt

After metals adsorption onto activated Ambersep® 900, a water wash was performed to evaluate its effectiveness in removing less desirable transition metals, such as Ti, Fe, and Zn (**Figure S9**) from the resin. The water wash effectively removed 100 % of Fe and Zn while allowing nearly 100 % of the Pt to remain adsorbed.

The stripping of Pt from the charged resin was achieved by testing several concentrations of thiourea solutions: 0.10 M, 0.25 M, 0.50 M, and 1.00 M. Thiourea was chosen as the stripping agent due to its strong affinity for PGM, attributed to the Lewis acid-base interaction. Specifically, Pt is classified as a soft acid and shows a preference for binding to soft bases such as the sulphur in thiourea, which contains large and polarizable donor atoms. Previous works have already reported the suceful use of this component to extract PGM from different types of adsorbents.[47,53–56] Even the most diluted thiourea solution (0.10 M) successfully extracted 100 % of the platinum adsorbed onto the resin (**Figure S10**). Considering the quantified metals in thiourea solution, Pt correspond of approximately 98 wt%, which is highly satisfactory for most applications.

4. Conceptual process and scale-up

The obtained results led to the conceptual development of a process that enables the extraction and recovery of PGM from SACC, illustrated in **Figure *9***. The process consists of three main stages: (1) pretreatment, (2) extraction and (3) purification. In **Figure 9**, the continuous arrows represent the steps developed in this work while the dashed lines represent conceptual steps that will be object of future study. Moreover, in each stage, the inlets and outlets are described with their composition, the global efficiency of Pt recovery or the resulting residues. Overall, to achieve a comprehensive process, it was

necessary to scale-up 60 times the study discussed in sections 3.2 and 3.3 in terms of leaching solution and mass of SACC (**Figure S11**), while some adaptations of the experiments and previously optimized conditions were needed (details can be found in the Supplementary Material).

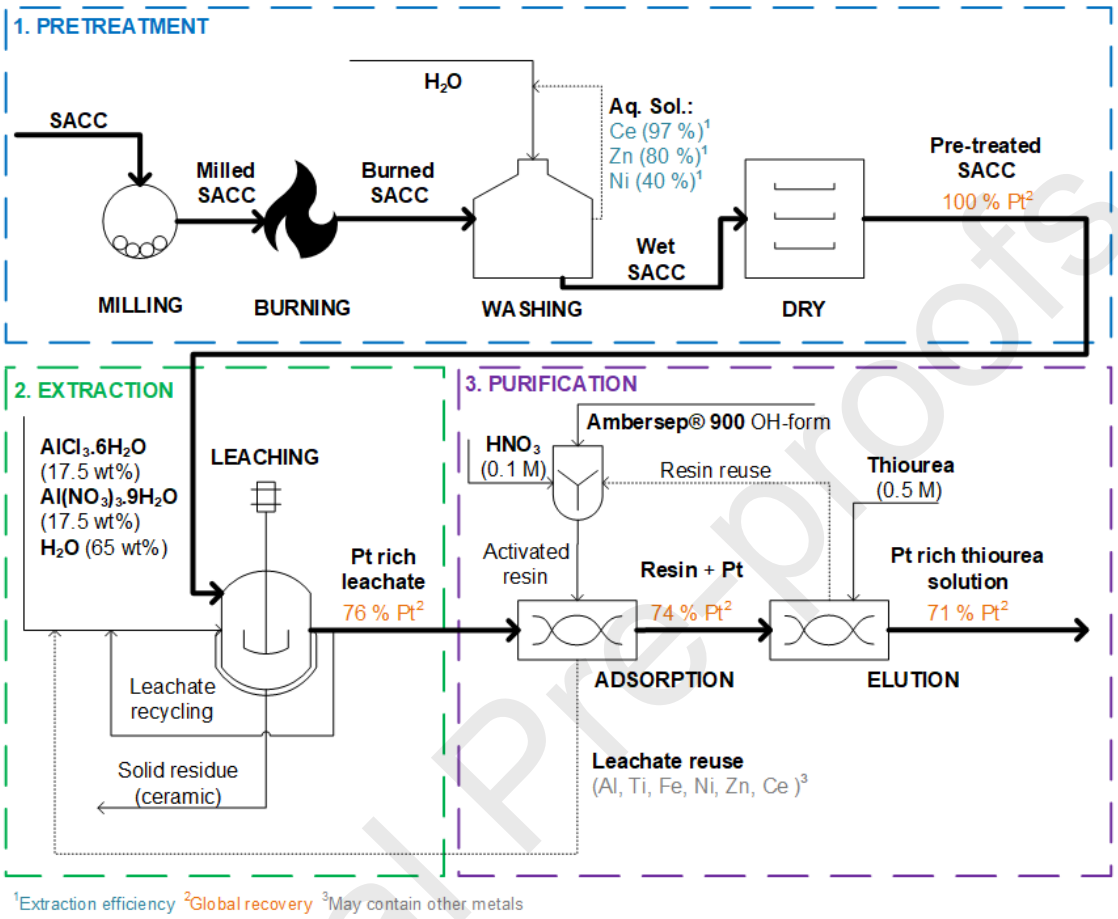

Figure 9. Process diagram of the selective recovery of Pt from real SACC by using Al-based salts solution.

As can be seen in **Figure 9**, the pretreatment, consists of milling, burning, and washing the SACC material. This step effectively reduces impurities, increasing the availability of Pt while removing metals such as nickel (40%), zinc (80 %), and cerium (97 %). To make this process more sustainable, future improvements could focus on reusing the aqueous solution generated during washing for multiple cycles. This reuse strategy could also facilitate the recovery of Ce.

For the extraction, a complementary study was conducted to evaluate the reuse of the leaching solution and to increase Pt concentration in the final leachate using the already optimized conditions. Five cycles were performed in total (**Figure S12**). The leaching solution maintained its extraction efficiency (EE_n) above 80 % throughout all cycles, demonstrating its reusability for at least five cycles, and potentially more. It was observed an increased extraction efficiency along the five cycles, with the last exceeding 100 % of extraction. This is likely due to evaporation of the leaching solution since system apparatus was not fully sealed. Additionally, the calculation of extraction efficiency was based on the initial volume of the leaching solution, which did not account for volume loss over time. To improve accuracy in future studies, the system should be fully enclosed to minimize evaporation.

This process produced a Pt-rich leachate with a concentration of (418 ± 3) $mg \cdot L^{-1}$, corresponding to a recovery of (76.5 ± 0.3)% of Pt relative to the total mass of SACC used across all five cycles. Although individual cycle extractions were higher, the final recovery was impacted by liquid losses inherent to the multistep process, including vial transfers, filtration, and other handling steps. A solid residue containing the remaining ceramic material from the SACC is also generated in this step.

In the third step, purification, the resin was able to effectively adsorb Pt at a R/L ratio of 1/100 w/w and contact time of 6 h (**Figure S13**) . The recovery of adsorption was (73.7 ± 0.1)% of the metal when comparing to the SACC composition. For the elution of the more concentrated leachate, a 0.5 M thiourea solution was needed to garatee 100 % desortion of Pt after a water wash of the resin (**Figure S14**), obtaining a final concentration of (407 ± 8) $mg.L^{-1}$ (**Figure S15** and **Figure S16**), which represents (96 ± 1) % of adsorbed Pt. Overall (71 ± 1) % of Pt present in catalyst was recovered from the thiourea solution. Some opportunities remain to increase the circularity of the process in this stage, including the use of the leachate solution after contact with the resin in more leaching steps, along with the reuse of the resin after reactivation.

The final product, a thiourea solution enriched with Pt, holds significant potential for direct use in the production of photocatalysts, such as those employed in hydrogen generation. Both thiourea and Pt are well-documented for their ability to enhance carbon-based photocatalysis for solar hydrogen production. [57,58] Future studies could explore the direct use of this leaching solution for Pt impregnation in photocatalysts, potentially replacing conventional processes and providing a more sustainable pathway to close the recycling loop and integrate PGM recovery into photocatalyst production. However, this investigation falls beyond the scope of the present study.

A preliminary cost-benefit assessment was performed to evaluate the economic potential of the proposed process, focusing on the reagent costs required to produce 1 L of Pt-containing leachate, as described in **Figure 9**. The reagents included are $AlCl_3 \cdot 6H_2O$, $Al(NO_3)_3 \cdot 9H_2O$, thiourea, HNO_3 and Ambersep® 900 OH-form resin, considering purchase prices for large volumes. [59,60] The total cost is €1.45 per litter, as shown in **Table 4**. The price and amount of Pt obtained is a key aspect to determine the viability of the process. The price considered was the average value for metallic Pt in 2024, 28.40 €/g.[8] The amount of Pt was calculated based on the final thiourea solution concentration (407 ± 8) $mg.L^{-1}$, worth €11.55. Overall, the process return was 10.10 €/L.

The reuse of the proposed leaching medium for five cycles demonstrates the economic viability of the suggested process, providing a margin of more than €10/L of solution. It is important to highlight that this study does not account for expenses related to labour, utilities (such as energy), administrative costs, or any other expenses associated with the overall operation of the process and proper treatment of waste effluents. Additionally, the possibility for the reuse for multiple times of the resin and thiourea solution is not considered and neither the reuse of the leaching solution after contact with the resin. Also, the return value represents a theoretical maximum return, assuming complete recovery and pricing based on metallic Pt. While metallic Pt is not the direct output of the process, the thiourea solution enriched with Pt may offer potential for direct application, avoiding additional purification steps and contributing to a more sustainable and economically viable recovery pathway. If further purification is required, it will depend on the intended application and the level of purity needed.

Table 4. Cost and return of the proposed process to recover Pt from SACC.[59,60]

Compound	Price (€/kg)	Consume/Production (kg/L)	Cost /return (€/L)
$AlCl_3 \cdot 6H_2O$	0.46	- 0.175	- 0.08
$Al(NO_3)_3 \cdot 9H_2O$	1.28	- 0.175	- 0.22
Resin	108	- 0.01	- 1.08
Thiourea	1.62	- 0.04	- 0.06
HNO_3	0.32	- 0.01	- 0.003
Pt	28400.17	+ 0.0004	+ 11.55
Balance			**+ 10.10**

5. Conclusion

This study presents a complete process for the selective recovery of Pt from a real SACC, covering all key stages from pretreatment, leaching, and selective separation to preliminary scale-up and economic evaluation. The new approach demonstrates the feasibility of developing sustainable hydrometallurgical routes for PGM recovery from real-world materials.

The SACC was initially pretreated by milling, burning and washing, which effectively eliminated impurities and improved Pt availability. For the extraction process, an efficient and scalable hydrometallurgical process was developed, offering an alternative to commonly used *aqua regia* solutions. The leaching was performed with a mixture of hydrated aluminum salts ($AlCl_3 \cdot 6H_2O$ and $Al(NO_3)_3 \cdot 9H_2O$). The parameters of the process were optimized to maximize Pt recovery while minimizing reagent consumption and included total salt concentration (35 wt %) and ratio ($AlCl_3 \cdot 6H_2O$ / $Al(NO_3)_3 \cdot 9H_2O$ = 1 w/w), solid-to-liquid ratio (1/20 w/w), and temperature (353 K). Temperature proved to be the key factor in the leaching of Pt and the mechanism of reaction was best described by the surface chemical reaction control model. Under these optimized conditions, a remarkably high Pt recovery efficiency of 94 % was achieved. The process was successfully scaled up 60-fold while maintaining leaching media reusability for at least five cycles and reaching 418 $mg.L^{-1}$ of Pt.

For the purification, Pt was selectively adsorbed by activated Ambersep® 900 anionic exchange resin, with a recovery rate of 97 % at the optimized R/L ratio of 1/100 w/w. The adsorption behaviour was best described by the Freundlich isotherm model, suggesting that Pt sorption occurs in multilayers on heterogeneous sites with interactions between adsorbate molecules. Kinetic analysis revealed that Ho's pseudo-second order (PSO) model provided a better fit than Lagergren's pseudo-first order (PFO) model. This indicates that chemisorption, involving valence forces and electron exchange or sharing between the resin and the metal, is the rate-limiting step in the process. For the elution, a thiourea solution was used and 96 % of the Pt adsorbed was recovered. Additionally, a preliminary cost analysis supports the economic viability of the process.

Overall, this process not only reduces the hazards associated with conventional acid PGM recovery methods but also promotes the circular economy by recovering valuable metals from end-of-life products. These findings provide a promising foundation for the industrial application of green chemistry in PGM recycling, addressing the urgent need for sustainable management of critical raw materials.

6. Acknowledgments

This work was financially supported by national funds through FCT – Fundação para a Ciência e a Tecnologia, I.P., within the scope of the project PlatILPlus (2022.04478.PTDC, DOI: 10.54499/2022.04478.PTDC). This work was financially supported by: UID/50020 of LSRE-LCM - Laboratory of Separation and Reaction Engineering – Laboratory of Catalysis and Materials - funded by Fundação para a Ciência e a Tecnologia, I.P. /MCTES through national funds; ALiCE, LA/P/0045/2020 (DOI: 10.54499/LA/P/0045/2020); and CICECO-Aveiro Institute of Materials, UIDB/50011/2020 (DOI: 10.54499/UIDB/50011/2020), UIDP/50011/2020 (DOI: 10.54499/UIDP/50011/2020) and LA/P/0006/2020 (DOI: 10.54499/LA/P/0006/2020). N. Schaeffer acknowledges the European Research Council (ERC) for the starting grant ERC-2023-StG-101116461. F.H.B. Sosa, A. R.F. Carreira and F. Braga acknowledge FCT for the researcher contract CEECIND/07209/2022 and the Ph.D. grants SFRH/BD/143612/2019 and 2023.01749.BD, respectively. The authors also acknowledge Valorcar – Sociedade de Gestão de Veículos em fim de Vida Lda. for providing the spent automotive catalytic converters.

7. References

[1] European Commission, Study on the critical raw materials for the EU 2023 – Final report, Publications Office of the European Union, 2023. https://doi.org/doi/10.2873/725585.

[2] International Platinum Group Metals Association (IPA), Catalytic converters: by how much do they reduce pollution?, (2012). https://ipa-news.com/index/pgm-applications/automotive/catalytic-converters/by-how-much-do-they-reduce-pollution.html?PHPSESSID=1eab3fd396c7cad1bbfe08bca4fae038 (accessed March 17, 2024).

[3] D. Yang, Q. Yang, W. Ma, X. Ma, S. Wang, Y. Lei, Characteristics of spent automotive catalytic converters and their effects on recycling platinum-group-metals and rare-earth-elements, Sep Purif Technol 308 (2023) 122977. https://doi.org/10.1016/j.seppur.2022.122977.

[4] O. Lanaridi, M. Schnürch, A. Limbeck, K. Schröder, Liquid- and solid-based separations employing ionic liquids for the recovery of Platinum Group Metals typically encountered in catalytic converters: a review, ChemSusChem 15 (2022) e202102262. https://doi.org/10.1002/cssc.202102262.

[5] J. Xia, A. Ghahreman, Platinum group metals recycling from spent automotive catalysts: metallurgical extraction and recovery technologies, Sep Purif Technol 311 (2023) 123357. https://doi.org/10.1016/j.seppur.2023.123357.

[6] N. Bahaloo-Horeh, S.M. Mousavi, Comprehensive characterization and environmental risk assessment of end-of-life automotive catalytic converters to arrange a sustainable roadmap for future recycling practices, J Hazard Mater 400 (2020) 123186. https://doi.org/10.1016/J.JHAZMAT.2020.123186.

[7] BloombergNEF (BNEF), Electric vehicle outlook 2023, 2023. https://assets.bbhub.io/professional/sites/24/2431510_BNEFElectricVehicleOutlook2023_ExecSummary.pdf (accessed May 14, 2024).

[8] Johnson Matthey, PGM prices and trading, (2024). http://www.platinum.matthey.com/prices/price-charts (accessed March 11, 2024).

[9] A. Cowley, PGM Market Report May 2023, Johnson Matthey Public Limited Company, 2023. https://doi.org/10.1595/205651323X16856083453770.

[10] United Nations Environment Programme (UNEP), Recycling rates of metals - A status report, 2011. https://www.resourcepanel.org/sites/default/files/documents/document/media/metals_status_report_full_report_english.pdf (accessed May 12, 2024).

[11] C. Zhang, F. Chen, S. Huang, S. Shen, Resource nationalism and platinum group metals: Chinese strategies in a hydrogen-powered future, Extr Ind Soc 15 (2023) 101317. https://doi.org/10.1016/J.EXIS.2023.101317.

[12] S.P. Singh, A.L. Schwan, Sulfur metabolism in plants and related biotechnologies, Comprehensive Biotechnology (2019) 221–236. https://doi.org/10.1016/B978-0-444-64046-8.00225-1.

[13] I. Chidunchi, M. Kulikov, R. Safarov, E. Kopishev, Extraction of platinum group metals from catalytic converters, Heliyon 10 (2024) e25283. https://doi.org/10.1016/J.HELIYON.2024.E25283.

[14] T. Abo Atia, J. Spooren, Fast microwave leaching of platinum, rhodium and cerium from spent non-milled autocatalyst monolith, Chemical Engineering and Processing - Process Intensification 164 (2021) 108378. https://doi.org/10.1016/J.CEP.2021.108378.

[15] I. Yakoumis, M. Panou, A.M. Moschovi, D. Panias, Recovery of platinum group metals from spent automotive catalysts: A review, Clean Eng Technol 3 (2021) 100112. https://doi.org/10.1016/j.clet.2021.100112.

[16] S. Karim, Y.P. Ting, Recycling pathways for platinum group metals from spent automotive catalyst: A review on conventional approaches and bio-processes, Resour Conserv Recycl 170 (2021) 105588. https://doi.org/10.1016/J.RESCONREC.2021.105588.

[17] M.K. Jha, J.C. Lee, M.S. Kim, J. Jeong, B.S. Kim, V. Kumar, Hydrometallurgical recovery/recycling of platinum by the leaching of spent catalysts: A review, Hydrometallurgy 133 (2013) 23–32. https://doi.org/10.1016/J.HYDROMET.2012.11.012.

[18] A. Ding, M. Li, C. Liu, X. Zhang, L. Lei, C. Xiao, Salt aqua regia as a green solvent for recovering precious metals, Cell Rep Phys Sci 3 (2022) 101159. https://doi.org/10.1016/j.xcrp.2022.101159.

[19] W. Lin, R.W. Zhang, S.S. Jang, C.P. Wong, J. Il Hong, "Organic aqua regia" - Powerful liquids for dissolving noble metals, Angewandte Chemie - International Edition 49 (2010) 7929–7932. https://doi.org/10.1002/anie.201001244.

[20] V.T. Nguyen, S. Riaño, E. Aktan, C. Deferm, J. Fransaer, K. Binnemans, Solvometallurgical recovery of platinum group metals from spent automotive catalysts, ACS Sustain Chem Eng 9 (2021) 337–350. https://doi.org/10.1021/acssuschemeng.0c07355.

[21] A. Nag, C.A. Morrison, J.B. Love, Rapid dissolution of noble metals in organic solvents, ChemSusChem 15 (2022). https://doi.org/10.1002/cssc.202201285.

[22] Y. Chen, M. Xu, J. Wen, Y. Wan, Q. Zhao, X. Cao, Y. Ding, Z.L. Wang, H. Li, Z. Bian, Selective recovery of precious metals through photocatalysis, Nat Sustain 4 (2021) 618–626. https://doi.org/10.1038/s41893-021-00697-4.

[23] D. Jimenez De Aberasturi, R. Pinedo, I. Ruiz De Larramendi, J.I. Ruiz De Larramendi, T. Rojo, Recovery by hydrometallurgical extraction of the platinum-group metals from car catalytic converters, Miner Eng 24 (2011) 505–513. https://doi.org/10.1016/J.MINENG.2010.12.009.

[24] Ş. Sarioğlan, Recovery of palladium from spent activated carbon-supported palladium catalysts, Platin Met Rev 57 (2013) 289–296. https://doi.org/10.1595/147106713X663988.

[25] S. Harjanto, Y. Cao, A. Shibayama, I. Naitoh, T. Nanami, K. Kasahara, Y. Okumura, K. Liu, T. Fujita, Leaching of Pt, Pd and Rh from automotive catalyst residue in various chloride based solutions, Mater Trans 47 (2006) 129–135.

[26] I. Yakoumis, A. Moschovi, M. Panou, D. Panias, Single-step hydrometallurgical method for the Platinum Group Metals leaching from commercial spent automotive catalysts, Journal of Sustainable Metallurgy 6 (2020) 259–268. https://doi.org/10.1007/s40831-020-00272-9.

[27] S. Ilyas, R.R. Srivastava, H. Kim, H.A. Cheema, Hydrometallurgical recycling of palladium and platinum from exhausted diesel oxidation catalysts, Sep Purif Technol 248 (2020) 117029. https://doi.org/10.1016/j.seppur.2020.117029.

[28] M. Mahmoud, Leaching Platinum-Group Metals in a sulfuric acid/chloride solution, JOM 55 (2003) 37–40. https://doi.org/https://doi.org/10.1007/s11837-003-0086-y.

[29] W. Liu, Y. Xu, Q. Yang, Y. Li, H. Xia, X. Wu, L. Zhang, Optimization of ultrasonic enhanced chloride-hydrogen peroxide system for leaching platinum from propane dehydrogenation spent catalyst by response surface methodology, Sep Purif Technol 353 (2025) 128384. https://doi.org/10.1016/j.seppur.2024.128384.

[30] T.N. Angelidis, E. Skouraki, Preliminary studies of platinum dissolution from a spent industrial catalyst, Appl Catal A Gen 142 (1996) 387–395. https://doi.org/10.1016/0926-860X(96)00088-9.

[31] R. Torres, G.T. Lapidus, Platinum, palladium and gold leaching from magnetite ore, with concentrated chloride solutions and ozone, Hydrometallurgy 166 (2016) 185–194. https://doi.org/10.1016/J.HYDROMET.2016.06.009.

[32] A. Ding, C. Liu, C. Xiao, Green palladium and platinum recovery by microwave-assisted aluminum chloride solution, Green Chemistry 26 (2024) 9220–9229. https://doi.org/10.1039/D4GC02503B.

[33] F. Forte, S. Riaño, K. Binnemans, Dissolution of noble metals in highly concentrated acidic salt solutions, Chemical Communications 56 (2020) 8230–8232. https://doi.org/10.1039/d0cc02298e.

[34] J.A. Duffy, M.D. Ingram, Metal aquo ions in molten salt hydrates. A new class of mineral acid?, Inorg Chem 16 (1977) 2988. https://doi.org/10.1021/ic50177a074.

[35] H.K. Chung, W.H. Kim, J. Park, J. Cho, T.Y. Jeong, P.K. Park, Application of Langmuir and Freundlich isotherms to predict adsorbate removal efficiency or required amount of adsorbent, Journal of Industrial and Engineering Chemistry 28 (2015) 241–246. https://doi.org/10.1016/J.JIEC.2015.02.021.

[36] M. Ozawa, Role of cerium–zirconium mixed oxides as catalysts for car pollution: A short review, J Alloys Compd 275–277 (1998) 886–890. https://doi.org/10.1016/S0925-8388(98)00477-0.

[37] Chasis & Body, Automotive catalytic converter market size, share & Covid impact analysis, 2023. https://www.fortunebusinessinsights.com/catalytic-converter-market-102046 (accessed March 10, 2024).

[38] S. Rauch, G.M. Morrison, M. Moldovan, Scanning laser ablation-ICP-MS tracking of platinum group elements in urban particles, Science of The Total Environment 286 (2002) 243–251. https://doi.org/10.1016/S0048-9697(01)00988-3.

[39] M. Omrani, M. Goriaux, Y. Liu, S. Martinet, L. Jean-Soro, V. Ruban, Platinum group elements study in automobile catalysts and exhaust gas samples, Environmental Pollution 257 (2020) 113477. https://doi.org/10.1016/J.ENVPOL.2019.113477.

[40] O. Šebek, M. Mihaljevič, L. Strnad, V. Ettler, J. Ježek, R. Štědrý, P. Drahota, L. Ackerman, V. Adamec, Dissolution kinetics of Pd and Pt from automobile catalysts by naturally occurring complexing agents, J Hazard Mater 198 (2011) 331–339. https://doi.org/10.1016/J.JHAZMAT.2011.10.051.

[41] X. Wei, C. Liu, H. Cao, P. Ning, W. Jin, Z. Yang, H. Wang, Z. Sun, Understanding the features of PGMs in spent ternary automobile catalysts for development of cleaner recovery technology, J Clean Prod 239 (2019) 118031. https://doi.org/10.1016/j.jclepro.2019.118031.

[42] L. Kong, Z. Wang, Z. Shi, X. Hu, A. Liu, W. Tao, B. Wang, Q. Wang, Leaching valuable metals from spent lithium-ion batteries using the reducing agent methanol, Environmental Science and Pollution Research 30 (2023) 4258–4268. https://doi.org/10.1007/s11356-022-22414-0.

[43] K.C. Liddell, Shrinking core models in hydrometallurgy: What students are not being told about the pseudo-steady approximation, Hydrometallurgy 79 (2005) 62–68. https://doi.org/10.1016/J.HYDROMET.2003.07.011.

[44] F. Faraji, A. Alizadeh, F. Rashchi, N. Mostoufi, Kinetics of leaching: A review, Reviews in Chemical Engineering 38 (2022) 113–148. https://doi.org/10.1515/revce-2019-0073.

[45] N.J. Bridges, K.E. Gutowski, R.D. Rogers, Investigation of aqueous biphasic systems formed from solutions of chaotropic salts with kosmotropic salts (salt–salt ABS), Green Chemistry 9 (2007) 177–18. https://doi.org/10.1039/b611628k.

[46] W. Kunz, J. Henle, B.W. Ninham, 'Zur Lehre von der Wirkung der Salze' (about the science of the effect of salts): Franz Hofmeister's historical papers, Curr Opin Colloid Interface Sci 9 (2004) 19–37. https://doi.org/10.1016/J.COCIS.2004.05.005.

[47] H. Zheng, Y. Ding, Q. Wen, B. Liu, S. Zhang, Separation and purification of platinum group metals from aqueous solution: Recent developments and industrial applications, Resour Conserv Recycl 167 (2021) 105417. https://doi.org/10.1016/J.RESCONREC.2021.105417.

[48] K. Shams, F. Goodarzi, Improved and selective platinum recovery from spent α-alumina supported catalysts using pretreated anionic ion exchange resin, J Hazard Mater 131 (2006) 229–237. https://doi.org/10.1016/J.JHAZMAT.2005.09.044.

[49] R.S. Marinho, C.N. da Silva, J.C. Afonso, J.W.S.D. da Cunha, Recovery of platinum, tin and indium from spent catalysts in chloride medium using strong basic anion exchange resins, J Hazard Mater 192 (2011) 1155–1160. https://doi.org/10.1016/J.JHAZMAT.2011.06.021.

[50] Y.S. Ho, G. McKay, Pseudo-second order model for sorption processes, Process Biochemistry 34 (1999) 451–465. https://doi.org/10.1016/S0032-9592(98)00112-5.

[51] H. Yuh-Shan, Citation review of Lagergren kinetic rate equation on adsorption reactions, Scientometrics 59 (2004) 171–177. https://doi.org/10.1023/B:SCIE.0000013305.99473.cf.

[52] N. Fatima, Q. Zhang, R. Chen, D. Yan, Q. Zhou, X. Lu, J. Xin, Adsorption thermodynamics and kinetics of resin for metal impurities in bis(2-hydroxyethyl) terephthalate, Polymers (Basel) 12 (2020) 2866. https://doi.org/10.3390/polym12122866.

[53] H. Zheng, Y. Ding, Q. Wen, B. Liu, S. Zhang, Separation and purification of platinum group metals from aqueous solution: Recent developments and industrial applications, Resour Conserv Recycl 167 (2021) 105417. https://doi.org/10.1016/J.RESCONREC.2021.105417.

[54] K. Fujiwara, A. Ramesh, T. Maki, H. Hasegawa, K. Ueda, Adsorption of platinum (IV), palladium (II) and gold (III) from aqueous solutions onto l-lysine modified

crosslinked chitosan resin, J Hazard Mater 146 (2007) 39–50. https://doi.org/10.1016/J.JHAZMAT.2006.11.049.

[55] A. Ramesh, H. Hasegawa, W. Sugimoto, T. Maki, K. Ueda, Adsorption of gold(III), platinum(IV) and palladium(II) onto glycine modified crosslinked chitosan resin, Bioresour Technol 99 (2008) 3801–3809. https://doi.org/10.1016/J.BIORTECH.2007.07.008.

[56] C. Xiong, Y. Zheng, Y. Feng, C. Yao, C. Ma, X. Zheng, J. Jiang, Preparation of a novel chloromethylated polystyrene-2-amino-1,3,4-thiadiazole chelating resin and its adsorption properties and mechanism for separation and recovery of Pt(iv) from aqueous solutions, J. Mater. Chem. A 2 (2014) 5379–5386. https://doi.org/10.1039/C3TA14923D.

[57] G. Zhang, J. Zhang, M. Zhang, X. Wang, Polycondensation of thiourea into carbon nitride semiconductors as visible light photocatalysts, J Mater Chem 22 (2012) 8083–8091. https://doi.org/10.1039/c2jm00097k.

[58] M. Kubovics, C.G. Silva, A.M. López-Periago, J.L. Faria, C. Domingo, Photocatalytic hydrogen production using porous 3D graphene-based aerogels supporting Pt/TiO2 nanoparticles, Gels 8 (2022). https://doi.org/10.3390/gels8110719.

[59] Made in China, (2024). https://www.made-in-china.com/ (accessed October 10, 2024).

[60] VWR, Ambersep® 900 (OH) Ion Exchange Resin (2024). https://pt.vwr.com/store/product/18041315/ambersep-900-oh-ion-exchange-resin (accessed October 11, 2024).

Graphical abstract

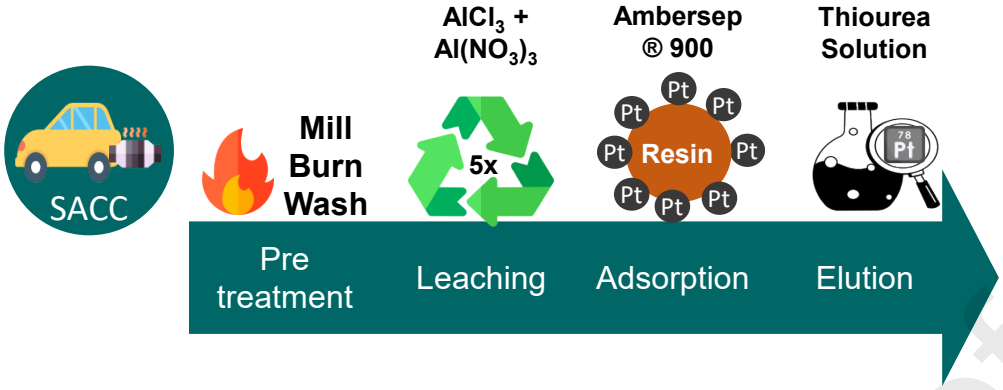

CRediT author statement

Flávia N. Braga: investigation, formal analysis, writing – original draft

António Coelho: investigation, formal analysis

Ana R. F. Carreira: investigation, formal analysis

Filipe H.B. Sosa: writing – review & editing, supervision

Nicolas Schaeffer: Conceptualization, methodology, writing – review & editing, supervision

Helena Passos: Conceptualization, methodology, writing – review & editing, supervision, funding acquisition

João A.P. Coutinho: Conceptualization, methodology, resources, writing – review & editing

Declaration of interests

☐ The authors declare that they have no known competing financial interests or personal relationships that could have appeared to influence the work reported in this paper.

☒ The authors declare the following financial interests/personal relationships which may be considered as potential competing interests:

Flavia N. Braga, Ana R.F. Carreira, Filipe H.B. Sosa reports financial support was provided by Foundation for Science and Technology. Nicolas Schaeffer reports financial support was provided by European Research Council. If there are other authors, they declare that they have no known competing financial interests or personal relationships that could have appeared to influence the work reported in this paper.